

APPENDIX X

MATES IV

FINAL REPORT

**The Spatial and Temporal Trends of
PM_{2.5}, PM₁₀, and TSP Components in the South Coast Air Basin**

Author

Kalam Cheung

Appendix X. The Spatial and Temporal Trends of PM_{2.5}, PM₁₀, and TSP Components in the South Coast Air Basin

X.1. Summary

To characterize the ambient level of toxic pollutants in the South Coast Air Basin, PM_{2.5}, PM₁₀ and Total Suspended Particles (TSP) samples are collected once every six days at 10 monitoring stations from July, 2012 to June, 2013. The spatial and seasonal trends of chemical components in PM_{2.5} are examined. Organic matter (OM) is the most dominant category, accounting for ~44% of the reconstructed mass, while approximately one-third (36%) is attributable to the group of inorganic ions. Elemental carbon (EC) contributes by 8.6%, followed by crustal materials (5.9%) and sea salt (5.3%). Due to limited atmospheric ventilation in cooler months, EC, OM and crustal materials concentrations are higher in the winter than in the summer in the source areas. In the inland receptor areas, regional transport is less pronounced in winter. Thus, their mass fractions in winter are generally similar to, or lower than those in summer. An air pollution episode occurred in early December, and fine particulate mass is elevated by $57 \pm 30\%$ across the Basin. In particular, the levels of EC, nitrate and ammonium are higher than the annual average by 2.5, 2.6 and 2.5 times, respectively. Overall, the levels of toxic air pollutants reduce considerably compared with MATES II and MATES III. Fine particulate EC is 36% lower than MATES III, due to reduction of tailpipe emissions. The decline is less pronounced (24%) for EC in PM₁₀. Additional analysis suggests that abrasion emissions induced by heavy-duty diesel vehicles may be a significant source of coarse PM-bound EC. For TSP, arsenic and cadmium concentrations are much lower than those observed in MATES II and MATES III, although the reductions are partly driven by the lower detection limits in the current study. Compared to MATES III, average levels of lead, nickel, vanadium, and hexavalent chromium decrease by 50, 36, 68 and 69% respectively.

X.2. Mass Reconstruction of PM_{2.5}

In the PM_{2.5} samples, levels of EC, organic carbon (OC), inorganic ions and metals are quantified. For the purpose of chemical mass reconstruction, these chemical components are grouped into five categories: EC, OM, crustal materials (CM), inorganic ions and sea salt. Reconstructed PM mass is calculated based on the sum of the five categories:

Reconstructed mass = elemental carbon + organic matter + crustal materials + inorganic ions + sea salt

EC is assumed to contain only carbon and requires no multiplier. OM is estimated from OC with a multiplier of 1.4 that accounts for the unmeasured hydrogen (H), oxygen (O), nitrogen (N), and sulfur (S) (Malm et al., 1994). Crustal materials (CM) consist of the typical geological materials including Al, Ca, Fe, Ti and Si. They are multiplied by 2.2, 1.63, 2.42, 1.94 and 2.49 respectively to account for the oxygen associated with these elements (Malm et al., 1994). Inorganic ions represent the sum of sulfate (SO_4^{2-}), nitrate (NO_3^-), and ammonium (NH_4^+). Previous studies in this Basin show that these are present in PM_{2.5} samples as ammonium sulfate ($(\text{NH}_4)_2\text{SO}_4$) and ammonium nitrate (NH_4NO_3); contributions from fugitive dust and salt are small,

and do not affect $PM_{2.5}$ mass reconstruction. Sea salt is estimated from the sum of sodium ion (Na^+) and chloride ion (Cl^-).

Daily reconstructed mass is calculated for each site and compared with gravimetric measurements. The reconstructed mass agrees well with the filter-based measurements ($R^2 = 0.69$, $n = 589$). The average ratio of reconstructed to gravimetric mass concentration is 1.03 ± 0.29 . The lower fraction occurs at the sampling stations of Anaheim (0.95 ± 0.19) and North Long Beach (0.91 ± 0.24). The uncertainty of the above-mentioned mass reconstruction method could be attributed to the uncertainty in the OC multiplication factor, which greatly depends on source characterization of organic component that may have consideration seasonal and spatial variation. Additionally, the higher relative humidity at coastal locations could hydrate particles during sample collection, which may still retain water content after equilibration at 30-40% relative humidity, thereby causing the discrepancy between the gravimetric and the reconstructed mass (Andrews et al., 2000).

Figure X-1 illustrates the chemical closure of $PM_{2.5}$. Overall, OM is the most dominant category, contributing an average of $44.2 \pm 1.0\%$ to the reconstructed mass. The levels of OM are relatively higher in sites that are further from the coast, namely Pico Rivera (annual avg. = $6.53 \mu g/m^3$), Burbank (annual avg. = $6.73 \mu g/m^3$), Inland Valley San Bernardino (annual avg. = $6.77 \mu g/m^3$) and Rubidoux (annual avg. = $6.47 \mu g/m^3$), although their contributions to the reconstruction mass are similar with other sites. The group of inorganic ions ($36.0 \pm 1.5\%$) is another major source category, with 16.0, 11.2 and 8.7% attributable to nitrate, sulfate and ammonia, respectively. EC accounts for an average of 8.6% of the reconstructed mass, and higher fractions are found at Pico Rivera (9.5%) and West Long Beach (9.3%). In general, the standard deviations of the site-wide annual average contribution of EC, OM and inorganic ions are less than 10% of their corresponding averages, highlighting the relatively low spatial variation of the three major source categories in this Basin. Approximately 5.9% of the reconstructed mass is attributed to crustal materials, with higher fractions at West Long Beach (8.1%) and Inland Valley San Bernardino (7.8%). Sea salt accounts for 5.3% of the reconstructed mass. Higher fractions are observed at West Long Beach (6.8%) and North Long Beach (7.2%), while the inland stations of Inland Valley San Bernardino and Rubidoux record lower fractions at 3.6% and 3.7%, respectively.

Meteorological conditions such as wind direction and speed, mixing height and temperature play an important role in the formation and removal mechanisms of PM components, thereby impacting ambient pollutant concentrations in different time of the year. EC shows a seasonal variation, with higher concentrations in winter (avg. = $1.88 \pm 1.2 \mu g/m^3$) than summer (avg. = $0.82 \pm 0.54 \mu g/m^3$). Such trend is more distinct in the source areas and less pronounced at the two inland sites. Mean monthly levels of EC in $PM_{2.5}$ ranged from 0.58 to $0.89 \mu g/m^3$ in summer to 1.34 to $2.15 \mu g/m^3$ in winter. In this Basin, EC predominantly arises from vehicular emissions. In winter, the level of atmospheric dispersion is generally lower due to lower temperature and weaker prevailing winds, facilitating the accumulation of air pollutants in the western side of the Basin. OM, predominantly arises from anthropogenic emissions in the fine mode, displays a similar seasonal trend with EC, with higher concentrations in winter (avg. = $6.93 \pm 2.7 \mu g/m^3$) than other seasons (avg. = $5.72 \pm 2.34 \mu g/m^3$). The seasonal characteristics of CM vary by location. At the two inland sites, winter CM levels are lower than or similar to those

of summer. At most other sites, CM levels are higher in winter than summer. Generally, sea salt levels are lower in winter (avg. = $0.52 \pm 0.43 \mu\text{g}/\text{m}^3$) than other seasons (avg. = $0.79 \pm 0.51 \mu\text{g}/\text{m}^3$). In this Basin, prevailing onshore wind is stronger in spring and summer, transporting marine emissions from the coast to the inland areas. The lower concentrations in winter result from the lower wind speed and the change of predominant wind direction (from westerly in summer to northerly and northeasterly in winter) in certain sites. The seasonal and spatial trend of inorganic ions is determined by sulfate, nitrate and ammonium. Winter sulfate levels are lower than summer levels by $77.7 \pm 4.6\%$. Across the 10 monitoring sites, winter concentrations range from 0.31 to $0.67 \mu\text{g}/\text{m}^3$, while summer levels vary from 1.95 to $2.39 \mu\text{g}/\text{m}^3$. The higher temperature in summer favors the photochemical oxidation of SO_2 and enhances the formation of particulate sulfate. Winter nitrate levels, on the other hand, are higher than or similar to those of summer. The seasonal variation is more distinct near the coast (North Long Beach, West Long Beach, Compton and Anaheim). Gas-to-particle conversion of ammonium nitrate is generally stronger in wintertime, when temperature is lower and more favorable for the formation of particulate nitrate (Seinfeld and Pandis, 2006). The seasonal variation of ammonium is similar to that of nitrate, with slightly higher concentration in winter than summer.

Note that an air pollution episode, defined as three or more continuous days of daily 24-hour average $\text{PM}_{2.5}$ concentration exceeding $35 \mu\text{g}/\text{m}^3$, occurred from December 7 to December 9, 2012. PM levels are elevated ($>30\%$ above annual average) from December 5 to December 11 at most sampling stations. As a result, the samples collected on December 5 and 11 of 2012 show considerably higher levels of PM components compared with other data collected in winter. Figure X-2 shows the chemical composition of $\text{PM}_{2.5}$ on December 11. Compared to the yearly averages (Figure X-1), the contributions of EC and inorganic ions to the reconstructed mass are higher on December 11, while the fractions of OM, crustal and sea salt decrease. Inorganic ion is the most abundant category, accounting for $43.0 \pm 3.1\%$ of the reconstructed mass. In particular, nitrate is a major constituent, and its contribution on December 11 (26.0%) is considerably higher than the yearly average contribution (16.0%). About one-third (35.8%) of the reconstructed mass is attributed to OM. EC's average contribution is $13.6 \pm 1.8\%$. Note that the episode is more pronounced at the source area, where both the gravimetric and reconstructed mass increase by more than 50% relative to the yearly averages. Given the spatial variation of the episode's magnitude, the increase levels of EC and inorganic ions in the source area, and the examination of meteorology (temperature, dew point, wind speed, etc.), the episode is likely due to an event of fog in stagnant conditions, which is characterized by an increase in relative humidity and reduction in atmospheric dilution. These atmospheric conditions favor the formation of secondary ions, resulting in their high concentrations in the source areas (Seinfeld and Pandis, 2006).

Chemical mass reconstruction is not conducted on PM_{10} and TSP measurement due to the absence of metal and/or inorganic ion data. Nonetheless, the ratios of EC and OC to gravimetric mass concentrations are compared. On average, EC accounts for $8.6 \pm 6.5\%$ and $5.9 \pm 3.1\%$ of $\text{PM}_{2.5}$ and PM_{10} , respectively. This is consistent with the understanding that EC is more abundant in fine PM than coarse PM in areas with dominant primary emissions. OC contributes to $33.7 \pm 14\%$ of $\text{PM}_{2.5}$ and $17.5 \pm 6.6\%$ of PM_{10} . The source of OC is distinct in the fine and coarse fraction in this Basin. OC in the fine mode primarily originates from anthropogenic emissions, while a significant fraction of coarse PM-bound OC arises from biogenic sources such

soil-derived dust and humic substances (Cheung et al., 2011). The mass fraction of OC in coarse mode aerosols is generally lower.

X.3. Elemental Carbon in PM_{2.5} and PM₁₀

EC was measured in both PM_{2.5} and PM₁₀ samples in the MATES III and MATES IV Study, while the MATES II Study quantified EC only in PM₁₀. Their levels are shown in Figures X-3 and X-4.

In the PM₁₀ samples, average EC level is $1.58 \pm 0.08 \mu\text{g}/\text{m}^3$. EC decreased by 24% compared to MATES III and 52% compared to MATES II. The reduction is more significant for fine particles. Average EC in PM_{2.5} is $1.17 \pm 0.99 \mu\text{g}/\text{m}^3$, which is 36% lower than MATES III. Fine particulate EC primarily arises from fossil fuel combustion in this Basin, whereas the contribution of biomass burning could be significant in the coarse mode in the inland areas, particularly in winter. Additionally, nonexhaust emissions, namely tire and brake wear, as well as road surface wear, could be a major source of EC in coarse PM. The higher reduction in fine particulate EC suggests the sources of EC in fine PM (i.e. emission from fossil fuel combustion) is more efficiently controlled than the sources in the coarse mode. Due to proximity to the Ports of Long Beach and Los Angeles, the two Long Beach sites are heavily influenced by heavy-duty diesel vehicle (HDDV). Although HDDV is a major source of EC, the levels of EC in Long Beach are similar to other monitoring sites, suggesting the reduction of tailpipe emissions of HDDVs and/or stronger dilution of air pollutants along the coast in MATES IV. In 2006, the Clean Air Action Plan was adopted by the Ports of Long Beach and Los Angeles. Incentives were provided to the trucking industry to switch to newer and cleaner trucks. Starting in 2012, trucks that do not meet the 2007 Federal Clean Truck Emission Standards are not allowed to service the Ports' terminals. The significant reductions of fine particulate EC at West Long Beach (44%), and to a lesser extent North Long Beach (38%), relative to MATES III are in line with the monitoring data from the ports. Note that the levels of some PM constituents measured at the MATES IV West Long Beach site were slightly higher than those measured concurrently at the MATES III West Long Beach site (more details about the location and comparison of the two sites can be found in Appendix V). Therefore, the percentage reduction of PM species from the ambient monitoring program in West Long Beach might be a low estimate.

On average, PM_{2.5}-bound EC contribute to 68% of the EC measured in the PM₁₀ samples. Interestingly, the ratio of PM_{2.5}-bound EC to PM₁₀-bound EC shows a spatial variation. The lower fractions at West Long Beach (57%) and North Long Beach (58%) indicate that a higher fraction of EC resides in the coarse mode at Long Beach compared to other areas. Wear from tires, brake, and road surface is a significant nonexhaust source of coarse particle emissions, particularly at Long Beach where HDDV is a major source of air pollutants. The lower ratios suggest that EC originating from HDDV, either as direct or indirect emissions, may contribute significantly to coarse particles. Additionally, the coarse fraction of EC, calculated as the difference between PM₁₀ and PM_{2.5}, is significantly higher at West Long Beach (avg. = $0.63 \mu\text{g}/\text{m}^3$; 95% CI = $0.08 \mu\text{g}/\text{m}^3$) than the nine other sites (avg. = $0.44 \mu\text{g}/\text{m}^3$; 95% CI = $0.03 \mu\text{g}/\text{m}^3$). West Long Beach is 100 m. east of the Terminal Island Freeway and 1.2 km. west of the Long Beach Freeway (I-710). It is heavily impacted by the large volume of HDDVs from port activity. Furthermore, the relative humidity is usually a few percent higher in Long Beach than

Central Los Angeles and the inland areas, thereby impeding the degree of particle re-suspension. The lower ratio at Long Beach suggests a local source, either in the form of emission or re-suspension of coarse particulate EC. HDDVs are known to have higher emissions of tire and brake wear due to the stronger abrasion processes, and they also induce a greater magnitude of particle re-suspension from the road than light-duty traffic (Charron and Harrison, 2005). Given that this site experiences similar fine particulate EC levels with other sites, it is likely that coarse PM-bound EC originate from the mechanical processes of abrasion from the HDDVs.

As mentioned previously, both PM_{2.5} and PM₁₀ EC levels are higher in winter than other seasons due to meteorology (Figures X-5 and X-6). During cooler months, the mixing height is generally lower. Furthermore, particle re-entrainment by wind reduces due to lower wind speed in the source area. Consequently, the effect of vehicle-induced re-suspension becomes more pronounced, resulting in higher fractions of traffic-related coarse particles. The seasonal trend is consistent at all sites with the exception of Central Los Angeles. PM_{2.5} EC winter level is 1.88 $\mu\text{g}/\text{m}^3$ (95% CI = 0.20 $\mu\text{g}/\text{m}^3$), doubling the average level of 0.93 $\mu\text{g}/\text{m}^3$ in other seasons (95% CI = 0.21 $\mu\text{g}/\text{m}^3$). Similar results are found for EC in PM₁₀. Winter average is 2.27 $\mu\text{g}/\text{m}^3$ (95% CI = 0.21 $\mu\text{g}/\text{m}^3$), compared with 1.34 $\mu\text{g}/\text{m}^3$ (95% CI = 0.07 $\mu\text{g}/\text{m}^3$) in other seasons.

X.4. Metals in TSP

Concentrations of selected metals in TSP in MATES IV, and their levels in MATES II and III, are shown in Figures X-7 to X-14.

Figures X-7 and X-8 show arsenic and cadmium concentrations. The average level of arsenic is 0.55 ng/m^3 , with higher levels at the inland areas. In Inland Valley San Bernardino, the average level is 0.91 ng/m^3 . In Rubidoux, the higher average of 0.76 ng/m^3 is driven by a spike of 6.34 ng/m^3 on July 14, 2012. Most measured elements recorded a considerably higher concentration (> 4 times higher than average) on that day. Note that the lower arsenic levels relative to MATES II is partly driven by the lower detection limits in the current study. The average concentration of cadmium is 0.16 ng/m^3 . Although MATES IV cadmium levels are considerably lower, these trends are largely due to the lower reporting limits for MATES IV (LOD = 0.08 ng/m^3), compared with the previous studies (LOD = 10 ng/m^3 for MATES II and 2 ng/m^3 for MATES III). Inland Valley San Bernardino records higher cadmium levels at an average of 0.28 ng/m^3 , followed by Central Los Angeles at 0.25 ng/m^3 . With the exception of Central Los Angeles and the two inland sites, cadmium levels are usually higher in winter than other seasons.

Figure X-9 shows the decline of lead, and the trend is consistent at all sites. Average lead concentration is 6.21 ng/m^3 , which is 50% lower than MATES III and 75% lower than MATES II. Inland Valley San Bernardino records higher lead levels at an average of 9.80 ng/m^3 , followed by Huntington Park at 9.46 ng/m^3 . The highest daily lead concentration of 81.7 ng/m^3 is observed at Huntington Park on February 15, 2013. All measured concentrations are below the Ambient Air Quality Standard of lead at 1,50 ng/m^3 .

Nickel and vanadium concentrations are shown in Figures X-10 and X-11. Compared with MATES III, vanadium reduces by 68% across the 10 sites, with higher reductions at Anaheim (80%), North Long Beach (78%) and West Long Beach (83%). The reduction of nickel is 36%, and the decline is again more pronounced at West Long Beach (67%), Anaheim (59%) and North

Long Beach (50%). Ni and V are impurities of bunker and fuel oil used in ships (Krudysz et al., 2008). Their declines at Long Beach suggest potential emissions reduction from ports activity. On the other hand, average nickel and vanadium concentrations are similar between MATES III and MATES IV at the two inland locations (Rubidoux and Inland Valley San Bernardino). Given their reductions at Long Beach, the higher levels at the inland sites suggest soil and road dust as a significant source of Ni and V in TSP. Nickel concentration is highest (avg. = 5.40 ng/m³) at Huntington Park, which is largely driven by a few data points in winter, as reflected in the higher confidence interval. With the exception of the two inland sites, winter nickel levels are higher than or similar to those of summer. Vanadium in fine PM could originate from oil combustion and industrial activities, while street and road dust is another source for coarser particles (Pakbin et al., 2011). Except for Anaheim, the level of vanadium is about two to four times higher in August (avg. = 9.05 ng/m³) than other months. Vanadium started to increase in late July, reached its peak in August, and declined in early September. Similar temporal trend is observed for other elements, namely, titanium, strontium, potassium, iron, molybdenum, copper, calcium, barium and zinc. Higher levels of windblown dust are usually observed in warmer months due to the stronger wind and lower relative humidity. The higher monthly concentration of vanadium and other crustal elements in August across the Basin could result from dust re-suspension.

Figure X-12 shows hexavalent chromium concentrations. In MATES II, half of the PM samples were analyzed by ARB and half were analyzed by SCAQMD. The ARB laboratory had higher method detection limits for hexavalent chromium, likely resulting in the lower reported concentrations than the SCAQMD samples. For comparison purposes, only results from the SCAQMD laboratory analyses are shown. Site-wide average hexavalent chromium level is 69% lower compared to MATES III. Winter levels are generally higher than other seasons. In particular, Compton and Huntington Park recorded higher concentrations on February 27, 2013, at 0.85 and 1.80 ng/m³, respectively. In MATES III, staff identified cement production as a source of elevated levels of hexavalent chromium near the Rubidoux site. In the current study, the annual average at Rubidoux is 0.041 ng/m³, lower than the levels at MATES III (avg. = 0.39 ng/m³) and the site-wide average of 0.056 ng/m³ in the current study.

Figures X-13 and X-14 illustrate the average level of selenium and manganese, both of which are in the EPA original list of hazardous air pollutants. In MATES III, all measured selenium levels were under the method detection limits of 2 ng/m³. For MATES IV, the average concentration is 0.82 ng/m³, with higher levels at Huntington Park (avg. = 1.67 ng/m³). The average concentration of manganese is 22.4 ng/m³. The highest average level is observed at Inland Valley San Bernardino (52.0 ng/m³), followed by Rubidoux (33.0 ng/m³). Overall, the reduction of manganese (28% relative to MATES III) is not as significant as other metals examined in this section. Manganese is an element in the upper continental crust. The high correlations (R² range from 0.60 to 0.93) between manganese and titanium, a dust tracer, suggesting that manganese in TSP primarily originates from crustal materials in this Basin. To examine the relative contributions of anthropogenic vs. crustal origins of manganese, crustal enrichment factors (CEFs) are calculated using the reference element of titanium. In brief, the level of observed manganese is divided by the level of observed titanium in this study, which is then normalized to the average abundance of manganese in the upper continental crust (UCC) obtained in Usher et al. (2006). Note that this calculation is typically conducted in reference to

aluminum, which is not quantified in TSP in this study. CEF > 10 is indicative of anthropogenic sources. Across the 10 sites, the average CEF range from 1.8 to 2.5. The highest CEF (10.9) is found at Compton on March 17, 2013. At the inland sites, all CEFs are below 5.

X.5. References

E. Andrews, P. Saxena, S. Musarra, L. M. Hildemann, P. Koutrakis, P. H. McMurry, I. Olmez, and W. H. White, Concentration and composition of atmospheric aerosols from the 1995 SEAVS experiment and a review of the closure between chemical and gravimetric measurements, *Journal of the Air & Waste Management Association*, 50, 5: 648-664, 2000.

A. Charron and R. M. Harrison, Fine (PM_{2.5}) and coarse (PM_{2.5-10}) particulate matter on a heavily trafficked London highway: Sources and processes, *Environmental Science & Technology*, 39, 20: 7768-7776, 2005.

K. Cheung, N. Daher, W. Kam, M. M. Shafer, Z. Ning, J. J. Schauer, and C. Sioutas, Spatial and temporal variation of chemical composition and mass closure of ambient coarse particulate matter (PM_{10-2.5}) in the Los Angeles area, *Atmospheric Environment*, 45, 16: 2651-2662, 2011.

M. A. Krudysz, J. R. Froines, P. M. Fine, and C. Sioutas, Intra-community spatial variation of size-fractionated PM mass, OC, EC, and trace elements in the Long Beach, CA area, *Atmospheric Environment*, 42, 21: 5374-5389, 2008.

W. C. Malm, J. F. Sisler, D. Huffman, R. A. Eldred, and T. A. Cahill, Spatial and seasonal trends in particle concentration and optical extinction in the United States, *Journal of Geophysical Research: Atmospheres*, 99, D1: 1347-1370, 1994.

P. Pakbin, Z. Ning, M. M. Shafer, J. J. Schauer, and C. Sioutas, Seasonal and Spatial Coarse Particle Elemental Concentrations in the Los Angeles Area, *Aerosol Science and Technology*, 45, 8: 949-U156, 2011.

J. H. Seinfeld and S. N. Pandis, *Atmospheric Chemistry and Physics - From Air Pollution to Climate Change*, (Second edition ed.), John Wiley & Sons, Inc, New York, 2006.

C.R. Usher, A. E. Michel and V.H. Grassian, Reactions on Mineral Dust, *Chemistry Reviews*, 103:4883-4939, 2003.

**Error bars in the charts denote 95% confidence interval*

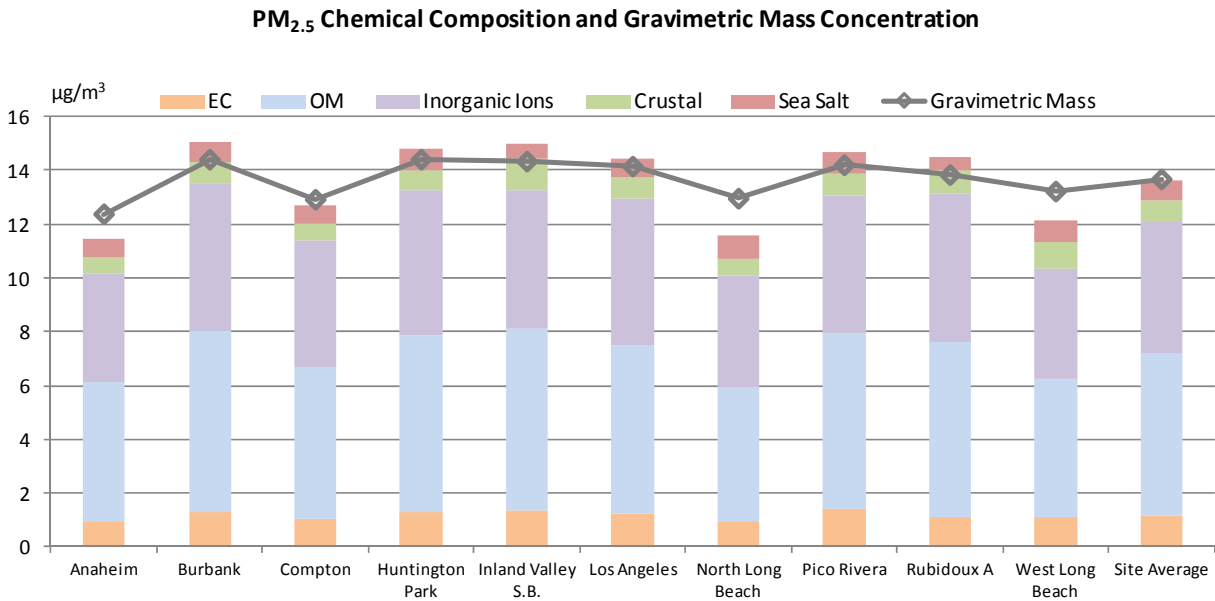


Figure X-1 Annual Average Chemical Composition and Gravimetric Mass Concentrations in PM_{2.5}

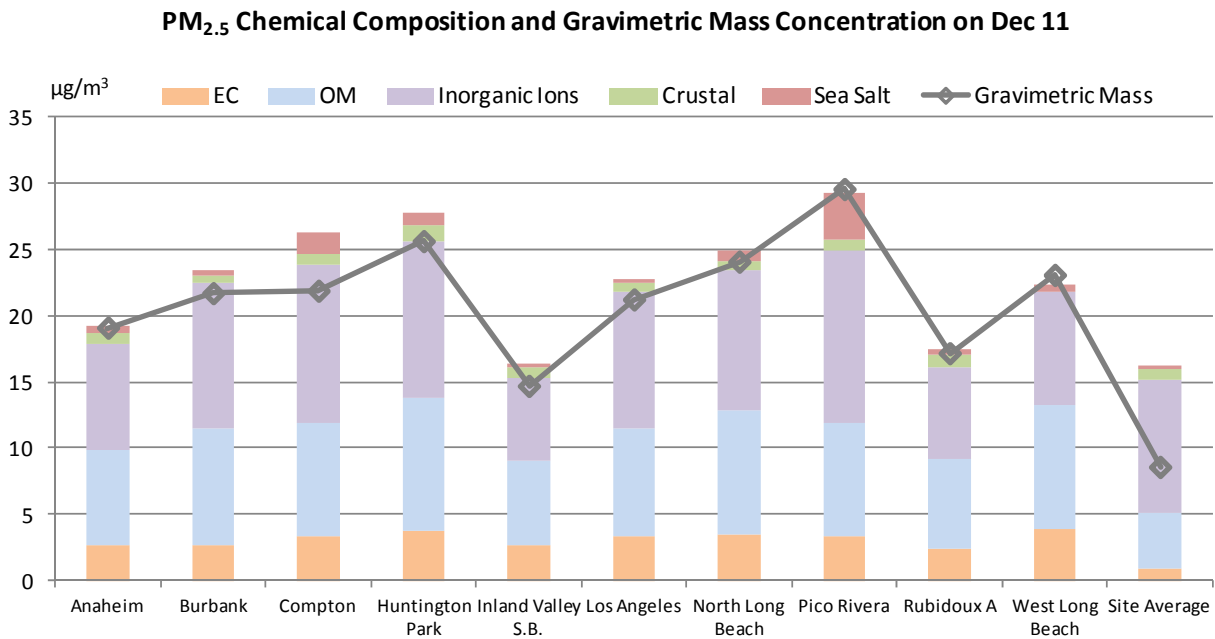


Figure X-2 Chemical Composition and Gravimetric Mass Concentrations in PM_{2.5} on December 11, 2012

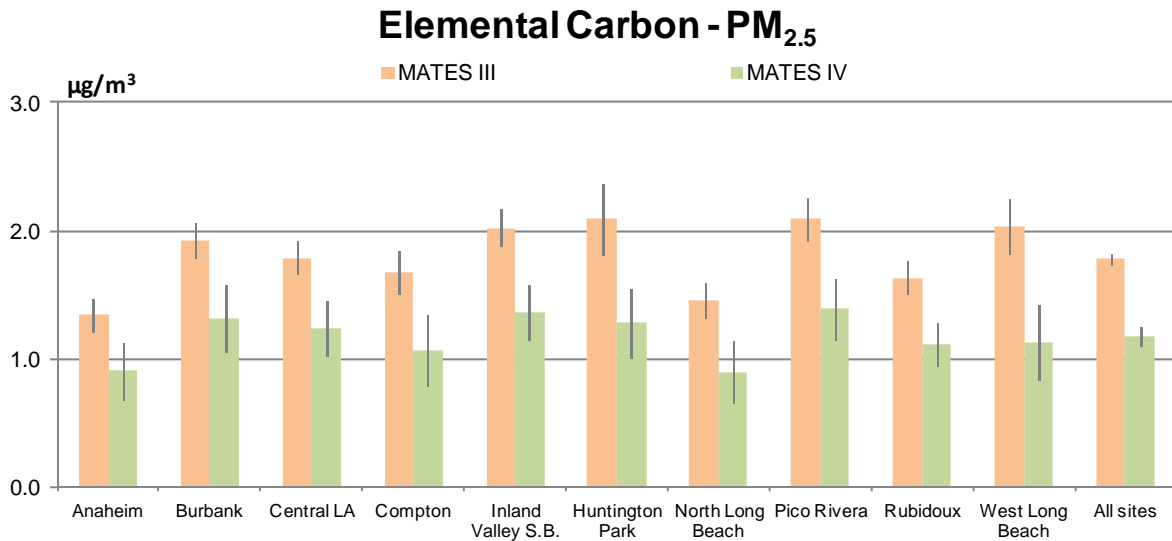


Figure X-3 Average Concentrations of Elemental Carbon in PM_{2.5}

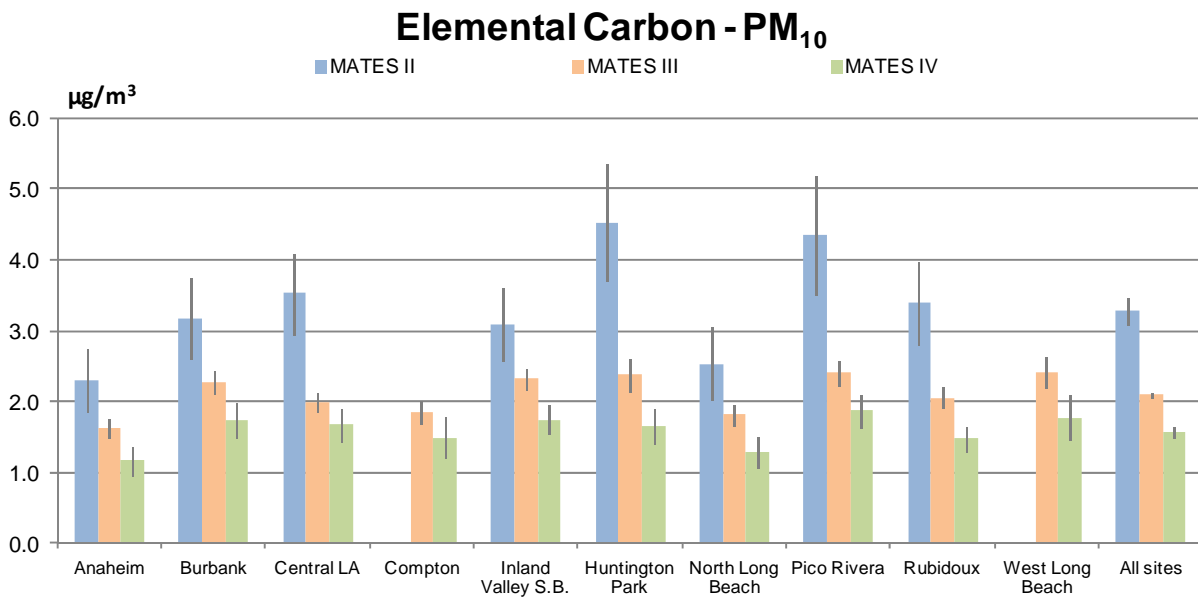


Figure X-4 Average Concentrations of Elemental Carbon in PM₁₀

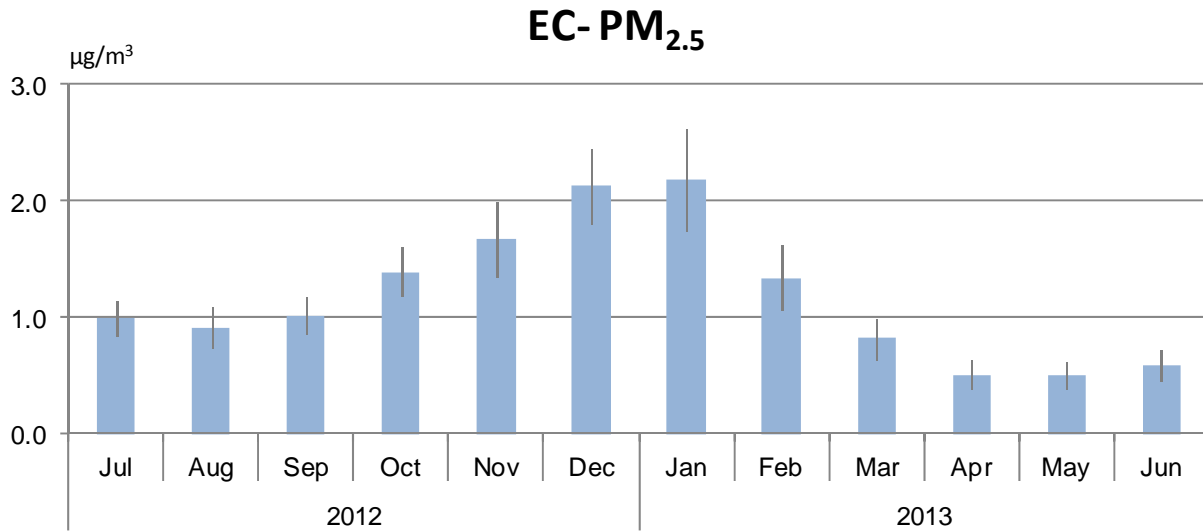


Figure X-5 Monthly Average Concentrations of Elemental Carbon in PM_{2.5}

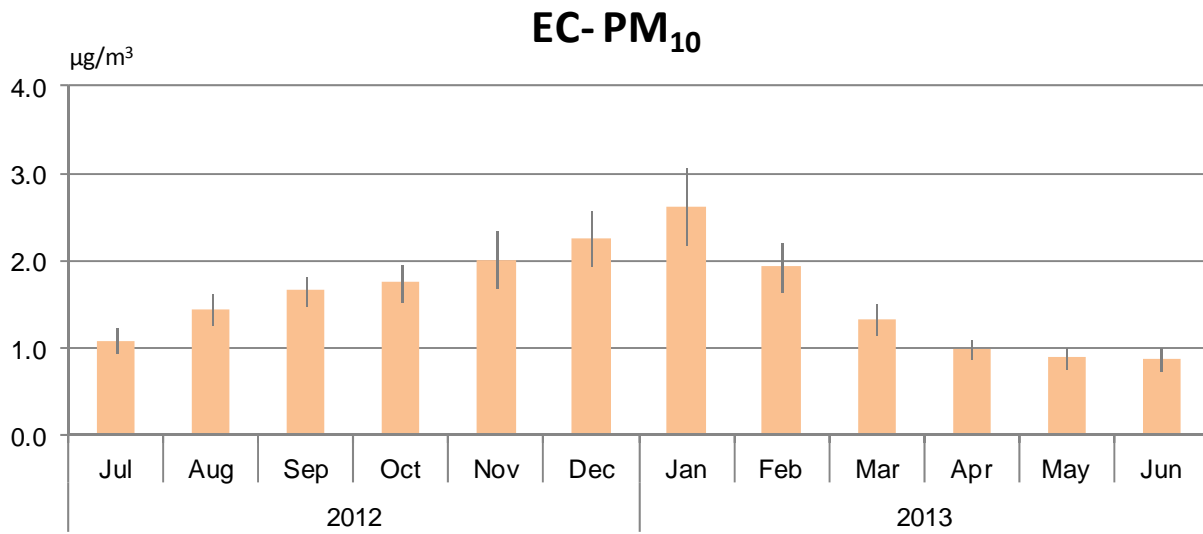


Figure X-6 Monthly Average Concentrations of Elemental Carbon in PM₁₀

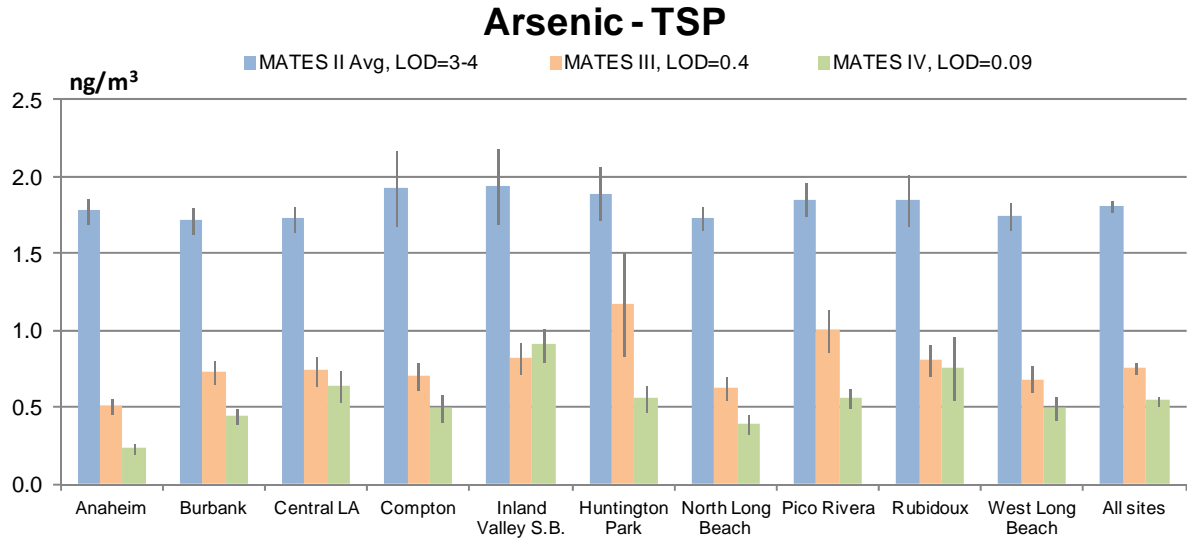


Figure X-7 Average Concentrations of Arsenic in Total Suspended Particulate (TSP)

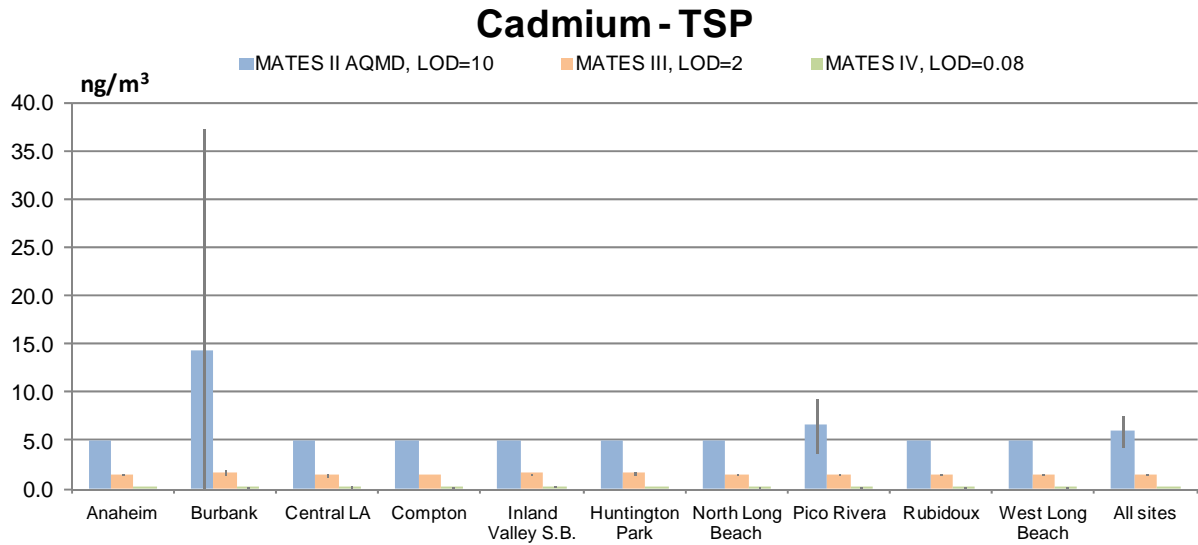


Figure X-8 Average Concentrations of Cadmium in Total Suspended Particulate (TSP)

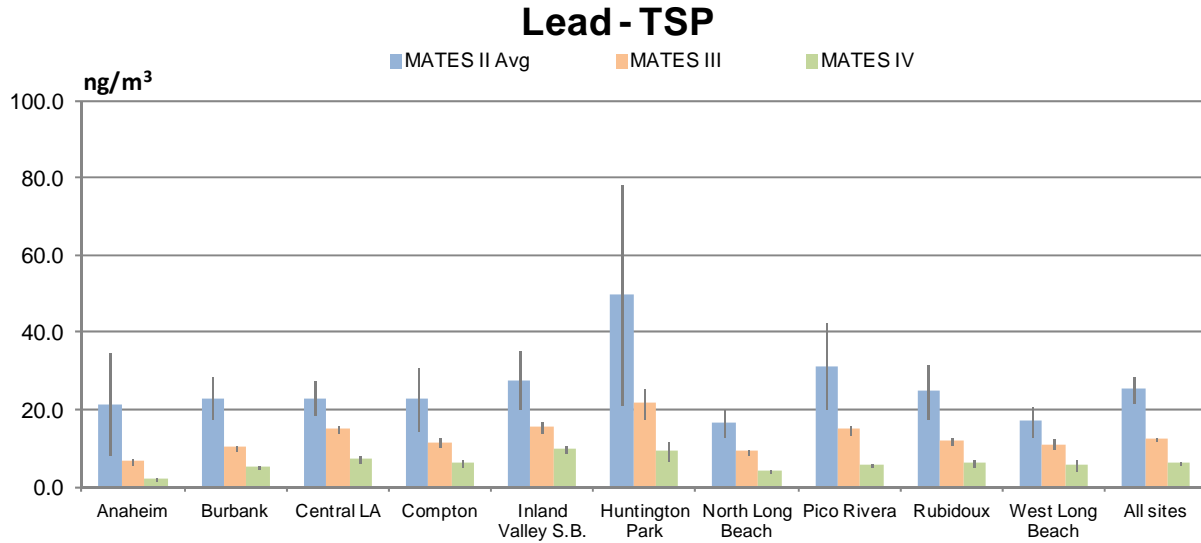


Figure X-9 Average Concentrations of Lead in Total Suspended Particulate (TSP)

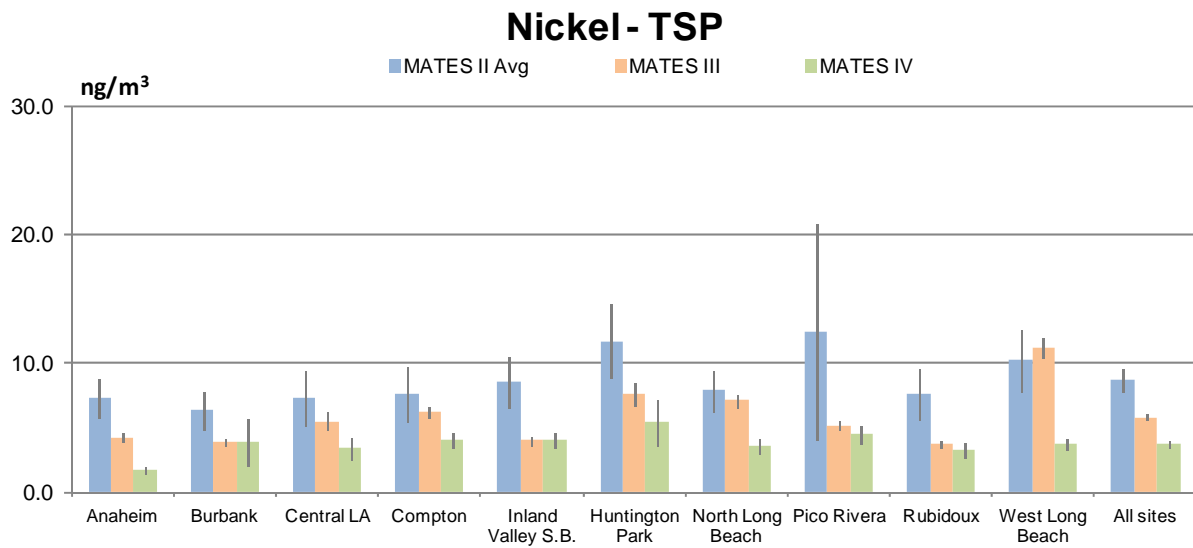


Figure X-10 Average Concentrations of Nickel in Total Suspended Particulate (TSP)

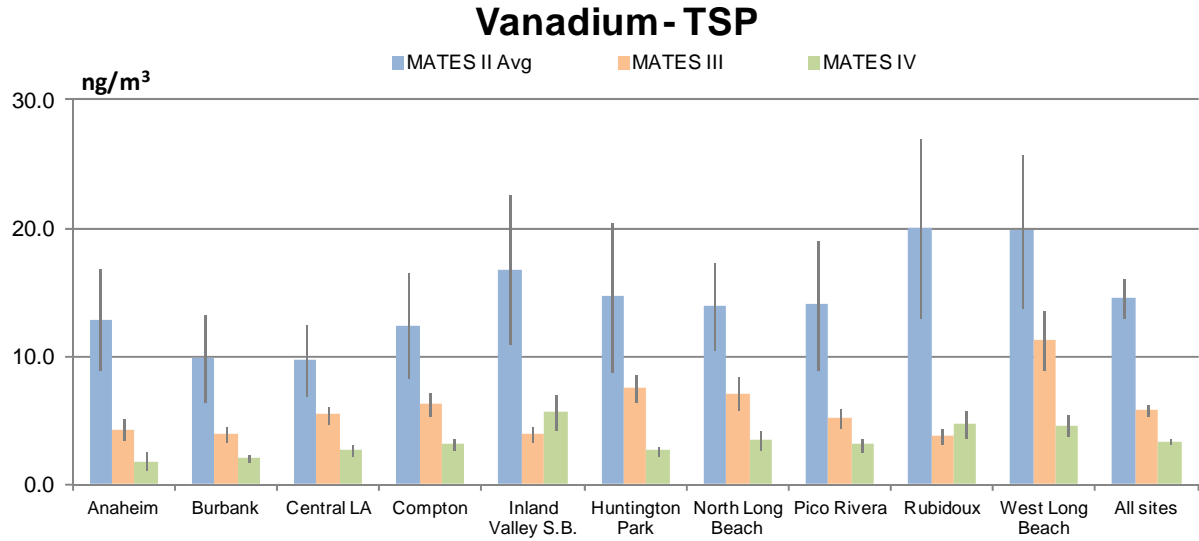


Figure X-11 Average Concentrations of Vanadium in Total Suspended Particulate (TSP)

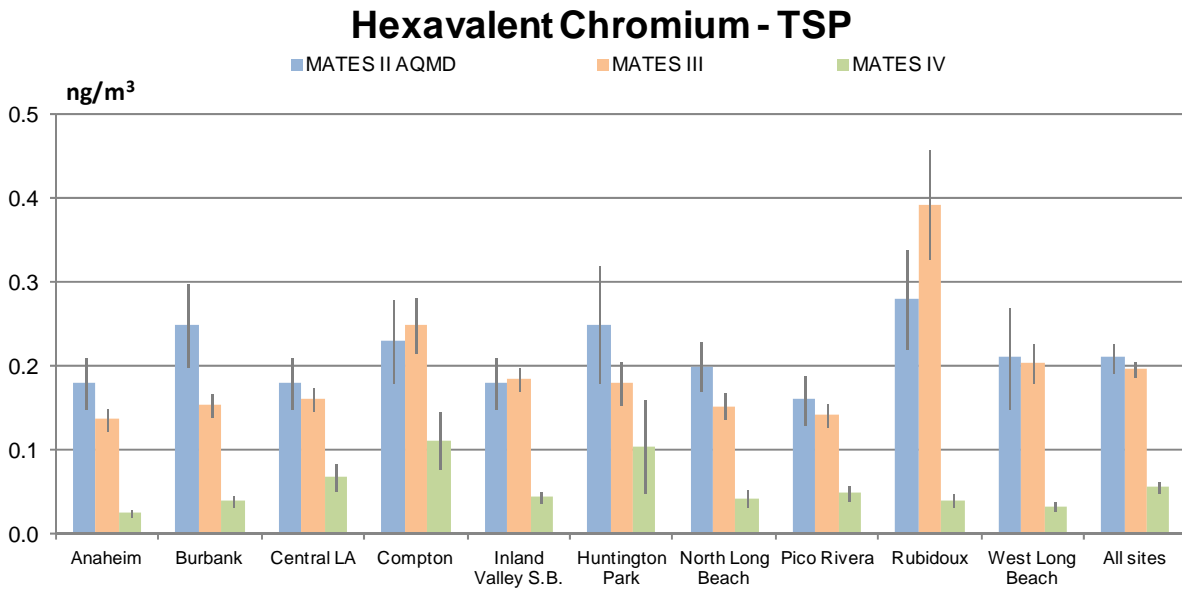


Figure X-12 Average Concentrations of Hexavalent Chromium in Total Suspended Particulate (TSP)

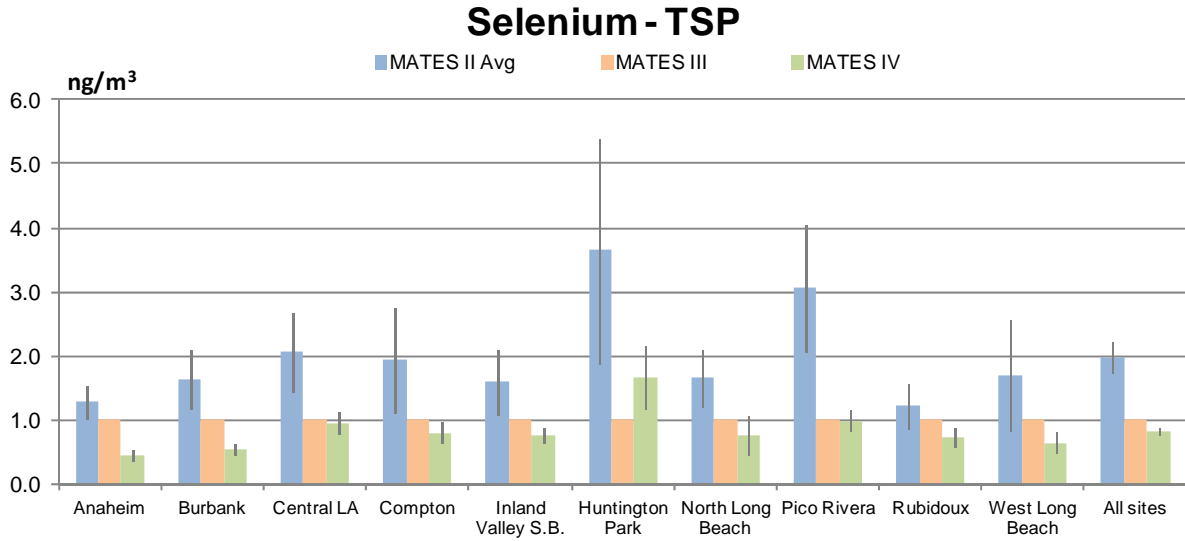


Figure X-13 Average Concentrations of Selenium in Total Suspended Particulate (TSP)

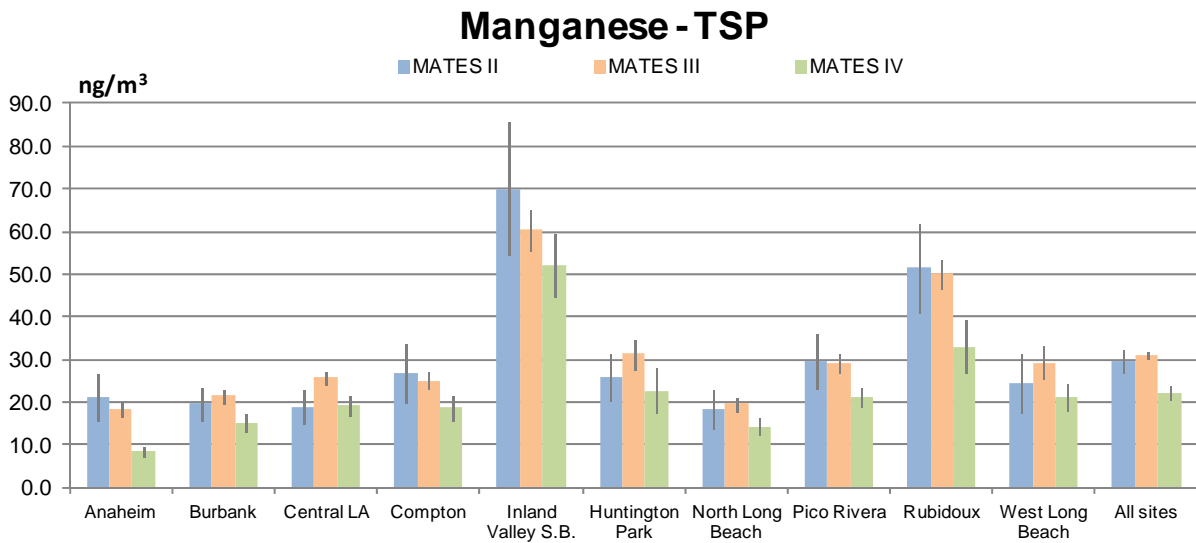


Figure X-14 Average Concentrations of Manganese in Total Suspended Particulate (TSP)